Supplementary Materials

Quantitative RT-PCR of Cxc chemokines with various signal inhibitors

To examine the underlying mechanism of Cxc chemokine upregulation by TGF-β blockade, we performed quantitative RT-PCR using the Kras+Tgfbr2^{KO} PDAC cells incubated with various representative signal inhibitors, including U1026 (Cell Signaling Technology) for ERK, LY294002 (Cell Signaling Technology) for PI3K, SP600125 (WAKO) for JNK, SB203580 (Cell Signaling Technology) for p38MAPK and SC-514 (Calbiochem) for NK-κB signal inhibition, respectively. The cells were incubated with or without 10 μM U0126, 10 μM LY294002, 10 μM SP600125, 10 μM SB203580, 50-100 μM SC-514, respectively, for 12 h, then RNA was extracted and subjected to QRT-PCR.

Knockdown of Cxcr2 in the Kras+Tgfbr2^{KO} PDAC cells and the pancreatic fibroblasts

pLKO.1-based lentiviral mouse Cxcr2 shRNA vector set was obtained from Open Biosystems. The non-target pLKO.1-scrambled shRNA (designated non-target-RNAi) was from Sigma. To prepare viral particles, 293T cells were co-transfected with 750 ng of psPAX2 packaging plasmid, 250 ng of pMD2.G envelope plasmid, and 2 μg of viral vector using Fugene6 (Roche Diagnostics). Supernatants containing lentivirus particles were collected 48 h of post-transfection and filtered.

For lentivirus infection, K399 (Kras+Tgfbr2KO PDAC cells) or K643f (pancreatic fibroblasts) cells in RPMI medium with 20% bovine serum and 8 μg/ml polybrene were incubated with an equal volume of lentivirus for 24 h. Stably transfected cells were selected in puromycin (3 μg/ml for K399, 30 μg/ml for K643f) and tested for Cxcr2 expression by QRT-PCR (Figure S3A).

Cxcr2 knockdown did not change in vitro cell proliferation and Cxcls expression neither in the K399 nor K643f, which were determined by Cell Counting kit-8 and quantitative RT-PCR as described in Methods (Figure S3B, D). On the other hand, Cxcr2 knockdown decreased Ctgf mRNA expression in the pancreatic fibroblasts (Figure S3C).

Apoptosis and cell proliferation assay in vivo

The Kras+Tgfbr2^{KO} mice were treated with gemcitabine, CXCR2 inhibitor (Repertaxin or SB225002), or gemcitabine + Repertaxin and euthanized at 7 weeks of age as described in the text. The PDAC tissue was fixed with 4% paraformaldehyde,

paraffin-embedded and subjected to examine apoptosis and cell proliferation in vivo. Apoptosis was examined by using Apoptag peroxidase in situ apoptosis detection kit (Chemicon International) according to the manufacturer's protocol. Apoptosis-positive tumor cells were counted among at least 1000 tumor cells in five randomly selected fields of each tissue. Tumor cell proliferation was examined by proliferating cell nuclear antigen (PCNA) immunohistocehmistry with anti-PCNA rabbit polyclonal antibody (FL-261, Santa Cruz Biotechnology, 1:200 dilution). PCNA labeling index was defined as a percentage of strong positive nuclear staining among 1000 tumor cells in five randomly selected fields of each tissue.

Figure legends for supplementary Figures

Figure S1. *Kras* and *Tgfbr2* allele recombination and ERK activation in the *Ptf1a$^{cre/+}$;LSL-Kras$^{G12D/+}$* mPanIN cells and *Ptf1a$^{cre/+}$;LSL-Kras$^{G12D/+}$;Tgfbr2$^{flox/flox}$* PDAC cells.

Genomic DNA PCR shows *Kras* allele recombination (upper band) both in the *Ptf1a$^{cre/+}$;LSL-Kras$^{G12D/+}$* mPanIN cells (K512 and K518) and *Ptf1a$^{cre/+}$;LSL-Kras$^{G12D/+}$;Tgfbr2$^{flox/flox}$* PDAC cells (K399) and *Tgfbr2* allele recombination only in the PDAC cells (K399). Western blot shows ERK1/2 phosphorylation (p-ERK1/2) both in the mPanIN and PDAC cells. (The lanes were run on the same gel but were noncontiguous.)

Figure S2. Screening of underlying signal mechanism of Cxc chemokine upregulation in the Kras+Tgfbr2^{KO} PDAC cells.

The Kras+Tgfbr2^{KO} PDAC cells (K375 and K399) were incubated with or without 10 μM U0126, 10 μM LY294002, 10 μM SP600125, 10 μM SB203580, respectively, for 12 h, then RNA was extracted and subjected to QRT-PCR of Cxcl1 and 5. The data without an inhibitor (control) is assigned as 1, and relative quantity is shown as mean ± SE, respectively. Cont: control, LY: LY294002, SB: SB203580, SP: SP600125.

Figure S3. Knockdown of Cxcr2 in the Kras+Tgfbr2^{KO} PDAC cells and pancreatic fibroblasts.

(A) Knockdown of Cxcr2 is confirmed in the Kras+Tgfbr2^{KO} PDAC cells (K399) and pancreatic fibroblasts (K643f) by QRT-PCR. The expression ratio of Cxcr2 to Gapdh is calculated. The data of control cells is assigned as 100% and relative expression is shown as mean ± SE. (B) Cxcr2 knockdown does not affect in vitro cell proliferation of K399 and K643f. (C) QRT-PCR shows that Cxcr2-knockdown decreases the Ctgf expression in the pancreatic fibroblasts. The expression ratio of Ctgf to Gapdh is calculated. The data of control fibroblasts is assigned as 1 and relative quantity is shown as mean ± SE. (D) QRT-PCR shows that Cxcr2-knockdown does not affect the Cxcl1 and 5 expression in the pancreatic fibroblasts. The data of control fibroblasts is assigned as 1 and relative quantity is shown as mean ± SE. Cont: control, KD: knockdown, *: $p<0.05$, ***: $p<0.001$ v.s. control, respectively.

Figure S4. Apoptosis and cell proliferation in the Kras+Tgfbr2^{KO} PDAC treated with gemcitabine and/or CXCR2 inhibitor in vivo.

(A) Apoptosis assay in vivo. The PDAC tissue was subjected to TUNEL-based apoptosis detection assay. The apoptosis-positive cells were counted among at least 1000 tumor cells in each tissue. (B) Cell proliferation assay in vivo. The PCNA immunohistochemistry was performed and PCNA labeling index was calculated as a percentage of PCNA-positive cells amoung 1000 tumor cells in each tissue. Bars: 100 μm. Mean $\pm$ SE is shown in the graphs. *: $p<0.05$, **: $p<0.01$, ***: $p<0.001$ v.s. control, respectively.

Figure S5. Survival of the Kras+Tgfbr2^{KO} PDAC mice treated with gemicitabine and/or CXCR2 inhibitor SB225002.

Survival curve of the Kras+Tgfbr2^{KO} PDAC mice treated with gemcitabine (blue), SB225002 (red), combination of the two (orange) or vehicle control (black). Logrank test shows that each treatment group has a statistically significant survival extension compared with the control group, but the survival of combination group does not show statistical difference from that of gemcitabine or SB225002 group. GEM+SB: gemcitabine + SB225002, MST: median survival time, *: $p<0.05$, ** $p<0.01$ v.s. control, respectively.

Table S1. A complete list of the molecules examined by cytokine antibody array

Il-1alpha, Il-1beta, Il-2, Il-3, Il-3rb, Il-4, Il-5, Il-6, Il-7, Il-9, Il-10, Il-12 p40, Il-12 p70, Il-13, Il-15, Il-17, Il-17br,
Ccl1, Ccl2, Ccl3, Ccl5, Ccl9, Ccl10, Ccl11, Ccl12, Ccl13, Ccl17, Ccl19, Ccl20, Ccl22, Ccl24, Ccl25, Ccl27,
Cxcl1, Cxcl2, Cxcl4, Cxcl5, Cxcl7, Cxcl9, Cxcl10, Cxcl11, Cxcl12, Cxcl13, Cxcl15, Cxcl16,
Cx3cl1, Xcl1,
Axl, CD26, CD30L, CD30T, CD40, Fasl, Gcsf, Gm-csf, M-csf, Ifngamma, Igf-I, Igf-II, Igfbp-2, Igfbp-3, Igfbp-5, Igfbp-6, Leptin, Lepr, L-selectin, P-selectin, E-selectin, Scf, Mmp-2, Mmp-3, Timp-1, Timp-2, pro-Mmp-9, Tnfalpha, sTnfrI, sTnfrII, Tpo, Vcam-1, Vegf, bFgf, Dtk, Fcgamma RIIb, Flt-3 ligand, Gitr, HGFR, Icam-1, Osteopontin, Osteoporotegerin, Resistin, Shh-n, Trance, Troy, Tslp, VEGFR1, VEGFR2, VEGFR3, Vegfd

Table S2. Sequences of primers for quantitative RT-PCR

Cxcl1:
5’ -CACCCAAACCGAAGTCATAG- 3’, 5’ -AAGCCAGCGTTCACCAGA- 3’
Cxcl5:
5’ -GGTCCACAGTGCCCTACG- 3’, 5’ -GCGAGTGCATTCCGCTTA- 3’
Cxcl16:
5’ -CGTTGTCCATTCTTTATCAGGTTCC- 3’, 5’ -TTGCGCTCAAAGCAGTCCA- 3’
Mmp2:
5’ -GACAAAGAGTTGGCAGTGC-3’, 5’ -CGGGTATCCATCTCCATGC- 3’
Cxcr2:
5’ -ATGCCCTCTATTCTGCCAGAT-3’, 5’ -GTGCTCCGGTTGTATAAGATGAC- 3’
Ctgf:
5’ -TGACTGCCCCTTCCCGAGAA-3’, 5’-TCTTCCAGTCGGTAGGCAGCTAGG- 3’
Gapdh:
5’ -CTGGCATGGCCTTCCGTG-3’, 5’ -GAAATGAGCTTGACAAAG-3’

Ijichi Fig. S1

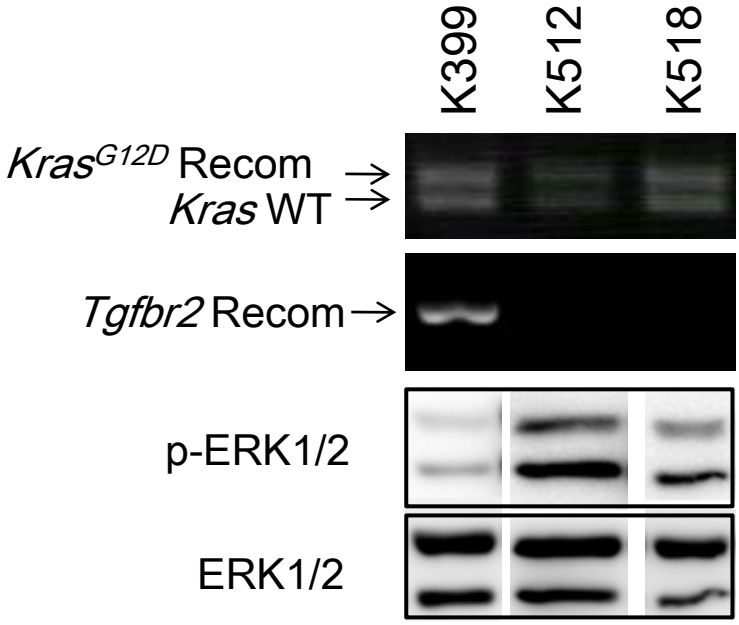

Ijichi Fig. S2

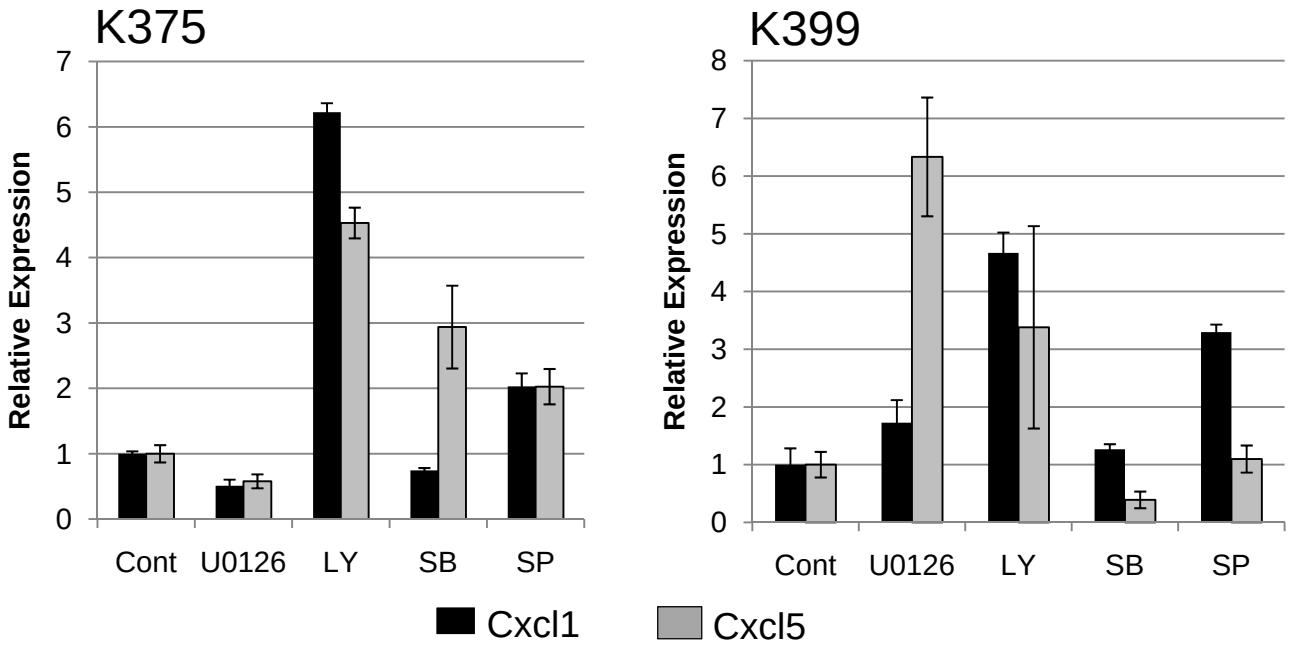

Ijichi Fig. S3

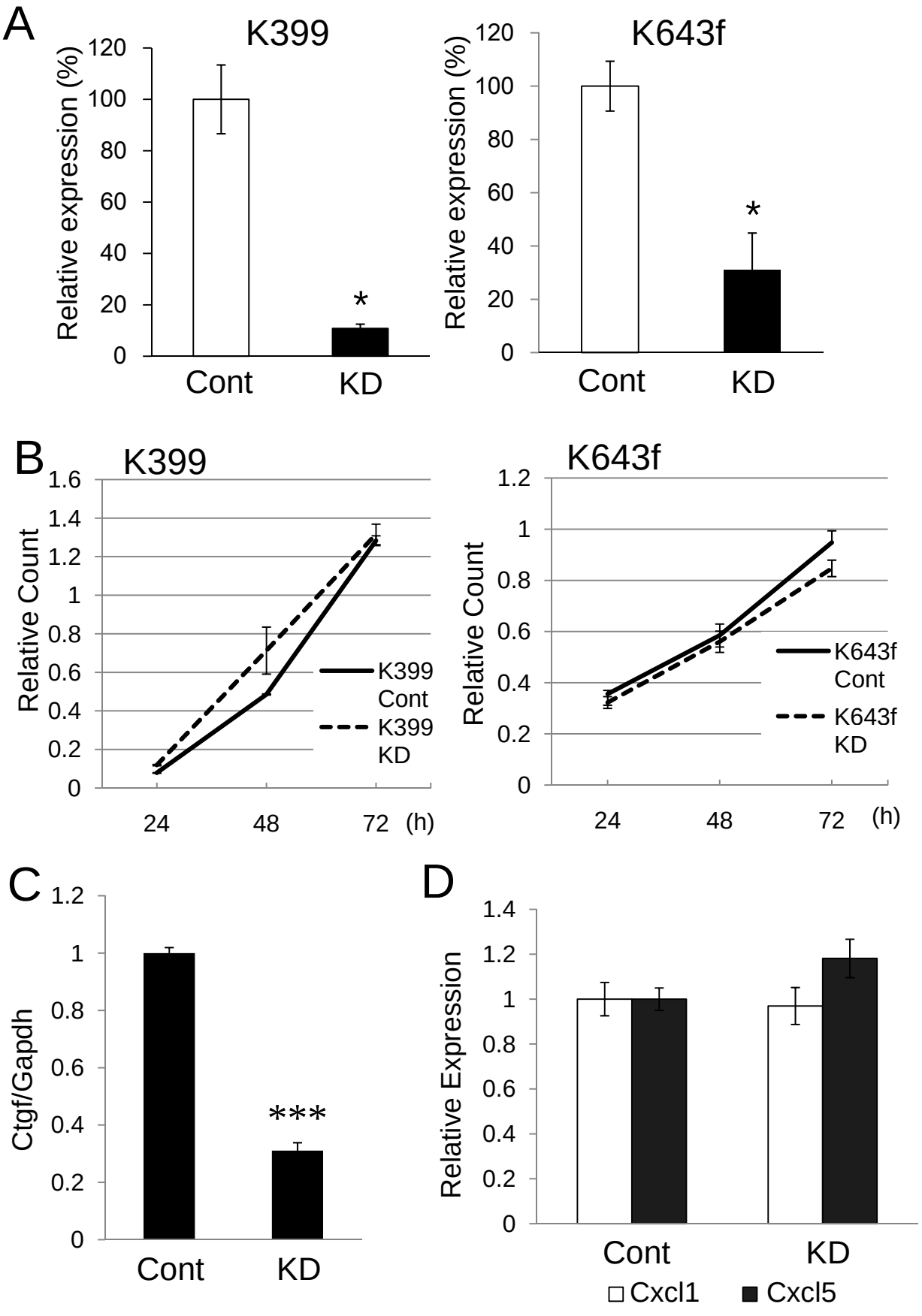

Ijichi Fig. S4

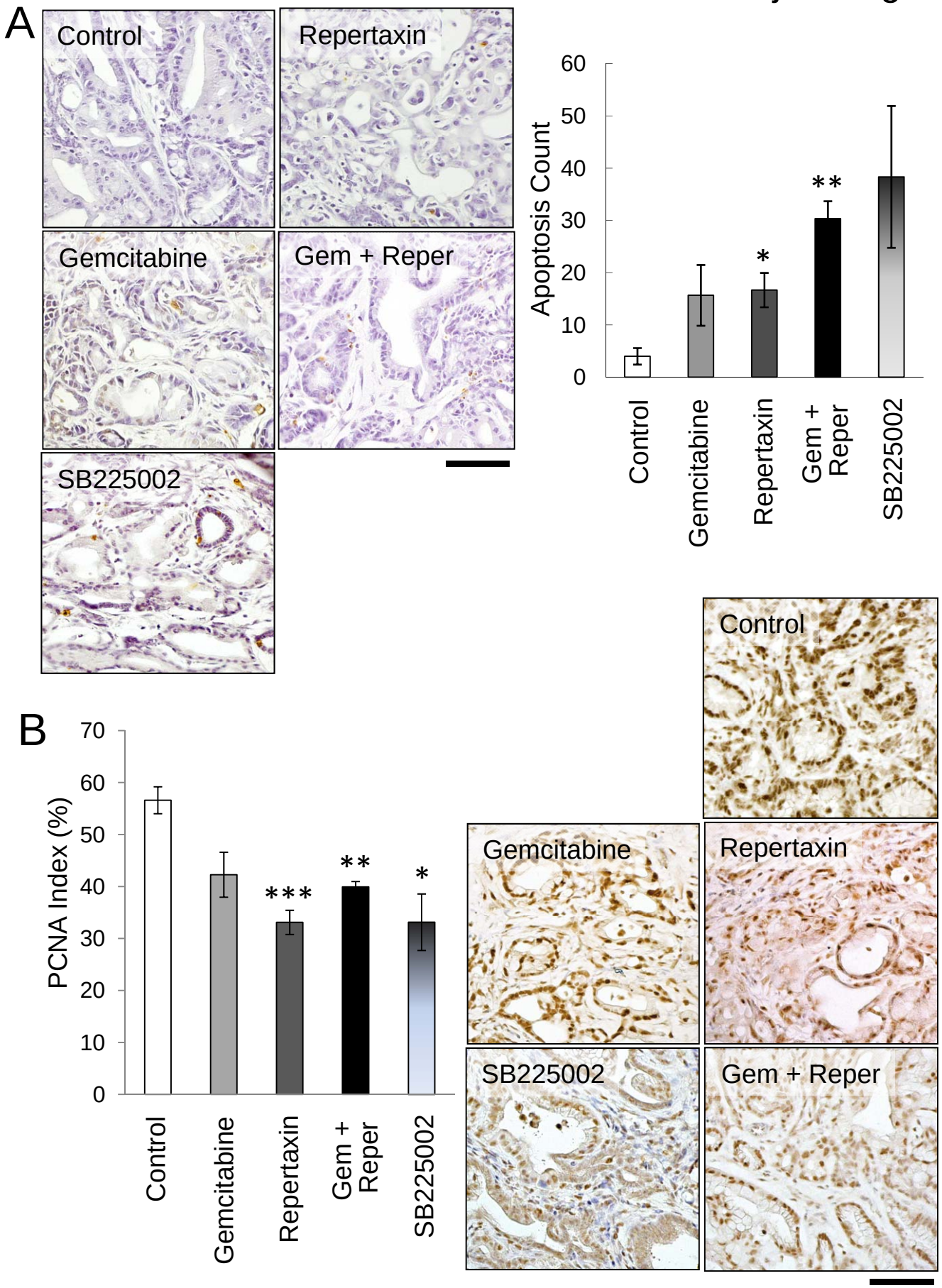

Ijichi Fig. S5